Colossal c-Axis Response and Lack of Rotational Symmetry Breaking within the Kagome Planes of the CsV_3Sb_5 Superconductor

Mehdi Frachet,[1,*] Liran Wang,[1] Wei Xia,[2,3] Yanfeng Guo,[2,3] Mingquan He,[4] Nour Maraytta,[1] Rolf Heid,[1] Amir-Abbas Haghighirad,[1] Michael Merz,[1,5] Christoph Meingast,[1,†] and Frédéric Hardy[1,‡]

[1]*Institute for Quantum Materials and Technologies, Karlsruhe Institute of Technology, D-76021 Karlsruhe, Germany*
[2]*School of Physical Science and Technology, ShanghaiTech University, Shanghai 201210, China*
[3]*ShanghaiTech Laboratory for Topological Physics, Shanghai 201210, China*
[4]*Low Temperature Physics Laboratory, College of Physics and Center of Quantum Materials and Devices, Chongqing University, Chongqing 401331, China*
[5]*Karlsruhe Nano Micro Facility (KNMFi), Karlsruhe Institute of Technology, 76344 Eggenstein-Leopoldshafen, Germany*

The kagome materials AV_3Sb_5 (A = K, Rb, Cs) host an intriguing interplay between unconventional superconductivity and charge-density waves. Here, we investigate CsV_3Sb_5 by combining high-resolution thermal-expansion, heat-capacity, and electrical resistance under strain measurements. We directly unveil that the superconducting and charge-ordered states strongly compete, and that this competition is dramatically influenced by tuning the crystallographic c axis. In addition, we report the absence of additional bulk phase transitions within the charge-ordered state, notably associated with rotational symmetry breaking within the kagome planes. This suggests that any breaking of the C_6 invariance occurs via different stacking of C_6-symmetric kagome patterns. Finally, we find that the charge-density-wave phase exhibits an enhanced A_{1g}-symmetric elastoresistance coefficient, whose large increase at low temperature is driven by electronic degrees of freedom.

The unique electronic band structure of delocalized electrons in kagome lattices features Dirac points, flat bands, and multiple van Hove singularities (vHS) close to the Fermi level [1]. Theoretical studies of kagome lattices demonstrate that the large density of state near van Hove filling can promote various exotic electronic orders, including charge-bond order, chiral charge-density wave, orbital-current order, and superconducting states of various gap symmetries [2–4].

In this context, the family of recently discovered kagome metals AV_3Sb_5 (A = K, Rb, Cs), crystallizing in the $P6/mmm$ hexagonal space group with perfect vanadium kagome networks, has emerged as an exciting realization of such physics with nontrivial topological properties, unconventional superconductivity, and intertwined symmetry-broken states [5,6]. Experimentally, two electronic instabilities are well established in all AV_3Sb_5, i.e., a charge-density wave (CDW) below $T_{CDW} \approx 94$ K, and bulk superconductivity (SC) that reaches $T_c \approx 2.5$ K in CsV_3Sb_5. The CDW state features a triple-$\mathbf{q}$-modulation with wave vectors connecting the three inequivalent sublattices and the corresponding M saddle points vHS. Below T_{CDW}, the translational symmetry of the crystal lattice is broken, but the c axis periodicity remains highly debated as, e.g., $2 \times 2 \times 2$ [7,8] and $2 \times 2 \times 4$ [9] superstructures, or a combination thereof [10,11], are reported.

The fate of the sixfold rotational invariance of the hexagonal lattice is controversial. Several experiments including x-ray diffraction (XRD), nuclear magnetic resonance (NMR), and scanning tunneling microscopy (STM) point to a lowering to C_2 rotational symmetry [11–14]. In addition, in CsV_3Sb_5, measurements of the electrical resistance under strain, namely elastoresistance, have been interpreted as an evidence for a growing electronic nematic susceptibility within the E_{2g} ($x^2 - y^2$) symmetry channel, ultimately leading to an ordered nematic state at $T_{nem} =$ 35 K [14,15]. However, different experiments suggest different critical temperatures for the C_6-symmetry breaking, ranging from T_{nem} to T_{CDW}. However, no thermodynamic evidence for such transition has been found and transport measurements on nearly-strain-free samples indicate that sixfold symmetry is preserved across the whole temperature range [16]. Further, conflicting results regarding a possible time-reversal symmetry breaking at T_{CDW} were reported [17–20], such that it remains unsettled whether AV_3Sb_5 could be the hosts of, e.g., a long-sought loop current order [19–21].

Although a conventional mechanism is unable to explain the superconducting state of AV_3Sb_5 [8], its nature remains unsettled. No consensus has been reached concerning the gap symmetry and the existence of gap nodes [22–24]. Further, it has been proposed that the SC and CDW states

conspire to form a pair-density wave [25], and, importantly, that electronic nematicity plays a key role in the mechanism of superconductivity in, e.g., $Cs(V_{1-x}Ti_x)_3Sb_5$ [15].

In this Letter, we use a powerful combination of bulk thermodynamic measurements, including high-resolution thermal expansion and heat capacity, with elastoresistance on CsV_3Sb_5 single crystals from two different sources to gain further insights into the CDW state and its connection with superconductivity. Our results directly demonstrate (i) a strong competition between the CDW and the SC states, dramatically influenced by c-axis tuning, (ii) the absence of an orthorhombic distortion for $T \leq T_{\mathrm{CDW}}$, implying that any sixfold symmetry breaking is largely decoupled from in-plane anisotropic strain and (iii) that the CDW is characterized by a strongly enhanced A_{1g}-symmetric elastoresistance, which further increases with decreasing temperature.

Single crystals of CsV_3Sb_5 were grown in Shanghai (batch A) and Karlsruhe (batch B) by the flux method and characterized by x-ray diffraction and energy-dispersive x-ray analysis (see Ref. [26]). In-plane thermal-expansion measurements were performed using a homebuilt high-resolution capacitive dilatometer on a large single crystal from batch A. Because of the large aspect ratio, c-axis measurements were performed using a stack of 20 smaller crystals from batch B, glued together with GE7031 varnish to a thickness of ≈2 mm. Elastoresistivity measurements were carried out by gluing samples from batch B on a piezoelectric stack (Pst 150/5x5/7 from Piezomechanik) using DevCon 5-min two-component epoxy (Part. No. X0039) as described in Ref. [27]. To extract the symmetry-resolved elastoresistance coefficients we assumed a temperature-independent Poisson ratio $\nu_p = -\epsilon_{yy}/\epsilon_{xx} \approx 0.43$ [28] for the piezoelectric stack (x is the poling direction). Heat-capacity measurements $C(\mathrm{T})$ were carried out on the same sample from batch A in a physical property measurement system from Quantum Design.

Figure 1(a) shows the relative length changes, $\Delta L/L$, of our sample as a function of temperature. A clear first-order discontinuity, for both a and c crystal axes (in the following, we use $P6/mmm$ space-group notations), accompanied by a large peak in the specific heat [see Fig. 1(e)] are observed at $T_{\mathrm{CDW}} \approx 93.5$ K, marking the transition to the CDW state. Although the CDW transition is clearly of first order, we also observe significant fluctuation effects both above and below the transition in an appropriate Grüneisen parameter (see Ref. [26]). At lower temperature, second-order discontinuities are clearly resolved at $T_c = 2.5$ K in both thermal-expansion coefficient, $\alpha_i(T) = 1/L_i(dL_i/dT)$ with $i = \{a, c\}$, and $C(\mathrm{T})$, as illustrated in Figs. 1(d) and 1(f), respectively. However, we find no evidence of a phase transition around 60 K [see Figs. 1(a) and 1(c)], especially in the c-axis thermal expansion, where sharp changes in the intensity of the superstructure reflections, accompanying the change of interlayer ordering, were observed by XRD [11]. This is rather surprising since band folding, resulting from a changing superstructure, is expected to substantially modify the Fermi surface and therefore the electronic entropy. Yet, no signature of this transition is resolved in either $C(T)$ or $\alpha(T)$, which measure the T and p derivative of the entropy, respectively.

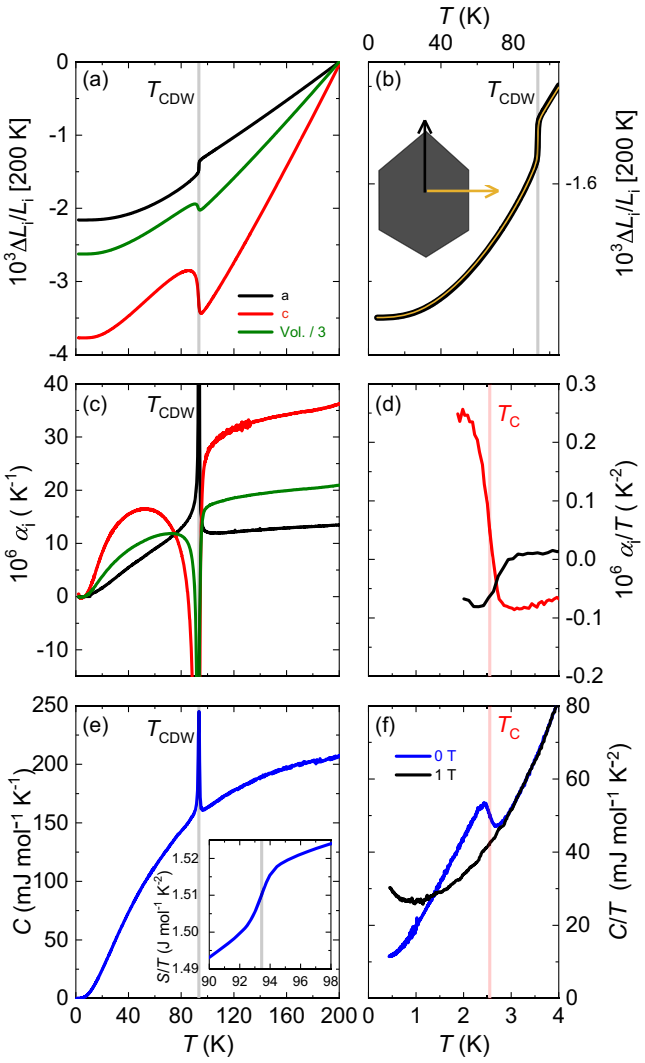

FIG. 1. (a) Relative length changes $\Delta L/L$ along the hexagonal directions and corresponding volume change as a function of temperature. The gray vertical line indicates T_{CDW}. (b) Comparison of $\Delta L_i/L_i$ measured along two orthogonal in-plane directions on the same single crystal. (c) Corresponding thermal-expansion coefficient, $\alpha = 1/L(dL/dT)$. (d) The thermal-expansion data for $T < 4$ K on a magnified view. (e) Heat capacity $C(T)$ showing the first-order transition at T_{CDW} and the corresponding entropy discontinuity (inset). (f) The superconducting transition in the specific heat on an extended view. The red vertical line indicates T_c.

Our measurements, however, clearly demonstrate a huge dependence of both CDW and SC on uniaxial pressure. Table I summarizes the initial uniaxial- and

TABLE I. Relative variations of T_c, T_{CDW}, and the Sommerfeld coefficient γ with uniaxial pressure along the a and c axes, calculated using the Ehrenfest, Clausius-Clapeyron, and Maxwell relations, respectively. The last column refers to the hydrostatic pressure dependence (see Ref. [26]).

	a	c	Volume
$d\ln T_c/dp_i$ (GPa^{-1})	−1.3	+4.7	+2.1
$d\ln T_{CDW}/dp_i$ (GPa^{-1})	+0.24	−1.3	−0.81
$d\ln\gamma/dp_i$ (GPa^{-1})	−0.06	+0.73	+0.58

hydrostatic-pressure dependences of T_{CDW} and T_c inferred from the application of the Clausius-Clapeyron and Ehrenfest relations (see Ref. [26]), respectively. The largest effect is found for the c axis where dT_{CDW}/dp_c amounts to $\approx -120\ \mathrm{K\,GPa}^{-1}$. This demonstrates that the large hydrostatic-pressure sensitivity of the CDW instability of CsV_3Sb_5 [40,41] originates predominantly from c-axis stress and highlights the importance of the apical Sb bonds and Sb-derived bands [42,43]. This is equally true for SC which also exhibits large uniaxial-pressure dependences but opposite in sign, confirming that both orders are competing for the same electronic states [29].

Remarkably, the relative change of T_c with c-axis stress, $1/T_c(dT_c/dp_c)$, is roughly a factor of 4 larger than that of T_{CDW}. Furthermore, the relative changes of the Sommerfeld coefficient γ and T_c with c-axis pressure are both positive. Thus, the increase of T_c under c-axis pressure is likely explained by an increase in the density of states due to the reduction of the CDW gap. Interestingly, this correlates with the convergence of M saddle points vHS toward the Fermi level [44].

Interestingly, we find no evidence for additional phase transition, in contrast to the reports of C_6-symmetry breaking at $T_{\mathrm{nem}} = 35$ K by elastoresistance and NMR [14,15], or directly below T_{CDW} by x-ray diffraction [11]. Such symmetry breaking should be detected using our high-resolution capacitive dilatometer by comparing the strains measured along two in-plane orthogonal directions [see Fig. 1(b)], as has been demonstrated for several Fe-based superconductors [45,46]. This is because our spring-loaded dilatometer exerts a non-negligible force of about 0.2 N along the measurement direction. Thus, for a measurement along directions perpendicular to the hexagonal faces (yellow curve), the population of possible structural domains with the shorter orthorhombic axis should be favored, resulting in an *in situ* detwinning of the sample below T_{CDW}, if the crystal symmetry were lowered. On the other hand, the twin population would remain unaffected by the applied force for measurements along the orthogonal direction (black curve), which probe a mixture of both orthorhombic axes. We find no discernible difference between the two measurements revealing the absence of in-plane orthorhombic distortion.

The lack of evidence for in-plane C_6-symmetry breaking in our thermal-expansion measurements motivates a closer inspection of the changes of electrical resistance, $\Delta R_{ii} = R_{ii}(\epsilon_{xx}) - R_{ii}(\epsilon_{xx} = 0)$ with $i = \{x, y\}$, in response to an applied strain ϵ_{xx}. Here, we induce a small symmetry-breaking strain to our crystals by gluing them on a piezostack [47], as depicted in the inset of Fig. 2(a), and we extract

$$\left(\frac{\Delta R}{R - R^0}\right)_{xx} - \left(\frac{\Delta R}{R - R^0}\right)_{\mathrm{yy}} = m_{\mathrm{E_{2g}}}(\epsilon_{xx} - \epsilon_{\mathrm{yy}}), \quad (1)$$

$$\left(\frac{\Delta R}{R - R^0}\right)_{xx} + \left(\frac{\Delta R}{R - R^0}\right)_{\mathrm{yy}} = m_{\mathrm{A_{1g}}}(\epsilon_{xx} + \epsilon_{\mathrm{yy}}), \quad (2)$$

where R^0 is the $T \to 0$ residual resistance and R_{xx} and R_{yy} correspond, respectively, to resistance measurements along and transverse to the poling direction. Hereafter, we denote them longitudinal and transverse measurements, respectively. $m_{\mathrm{A_{1g}}}$ and $m_{\mathrm{E_{2g}}}$ represent the respective elastoresistance coefficients that transform according to the A_{1g} and E_{2g} irreducible representations of the D_{6h} point group (see Ref. [26]). We note that the quite large resistivity anisotropy $(\rho_c/\rho_{ab})(50\ \mathrm{K}) \approx 25$ in CsV_3Sb_5 implies that our transport data are dominated by the in-plane response [13].

In Fig. 2, we report the results of our elastoresistance measurements on CsV_3Sb_5 (see Ref. [26]). The linear slopes $(dR_{ii}/d\epsilon_{xx})$ of the resistance-vs-strain curves normalized by the total R_{ii} and $(R_{ii} - R^0_{ii})$ are compared in Fig. 2(a). At lower temperatures the effect of normalization by R^0_{ii} makes a huge difference and is necessary to obtain physically meaningful results, as discussed in Ref. [48]. For $T > T_{\mathrm{CDW}}$, the strain response is weakly temperature dependent and amounts to ≈2–4, as expected in any metals. At $T \approx T_{\mathrm{CDW}}$, a sharp peak is resolved in both directions. This peak, that has not been resolved in any AV_3Sb_5 [14,15] is, however, naturally expected given the strong uniaxial-pressure dependence of T_{CDW} according to

$$\left(\frac{dR}{d\epsilon_{xx}}\right)_{T_{\mathrm{CDW}}} \propto \left(\frac{\partial R}{\partial T}\right)_{T_{\mathrm{CDW}}} \left(\frac{dT_{\mathrm{CDW}}}{dp_a}\right). \quad (3)$$

The validity of Eq. (3) is provided by the essentially similar strain conditions achieved under uniaxial pressure and in-plane biaxial and anisotropic strain induced by the piezostack (see details in [26]). Thus, a positive elastoresistance peak implies that $dT_{\mathrm{CDW}}/dp_a > 0$, in excellent agreement with our thermal-expansion measurements (see Table I) and previous direct uniaxial-stress experiments [29].

For $T \lesssim T_{\mathrm{CDW}}$, the elastoresistance does not turn back to a typical metallic value. It is rather significantly enhanced [14,15] for both longitudinal and transverse

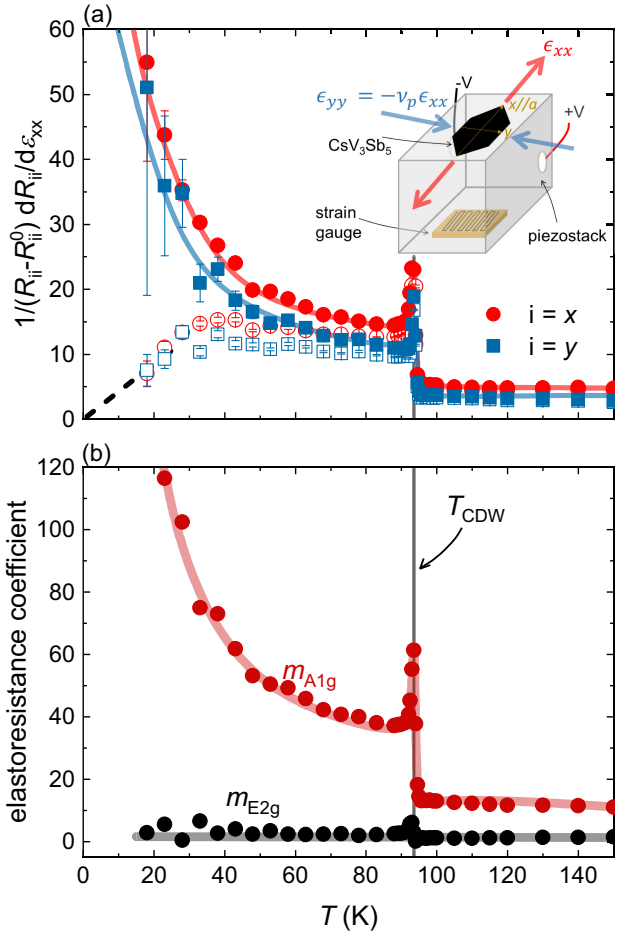

FIG. 2. (a) Linear slopes of the resistance versus strain curves, $1/(R_{ii} - R^0)(dR_{ii}/d\epsilon_{xx})$, in the longitudinal ($i = x$, red symbols) and transverse ($i = y$, blue symbols) channels. The empty symbols correspond to resistance variation relative to the total resistance (including the residual term), $1/R_{ii}(dR_{ii}/d\epsilon_{xx})$, as discussed in earlier works [14,15]. The inset shows a sketch of the experimental setup with the sample (black) glued on the top side of a piezoelectric stack (gray) with the crystallographic a axis aligned along the poling direction (x). (b) Corresponding E_{2g} and A_{1g} symmetry-resolved elastoresistance coefficients. The vertical line indicates T_{CDW}.

channels, as illustrated in Fig. 2(a). Hence, the electronic properties of CsV_3Sb_5 in the CDW state are mainly sensitive to a symmetry-preserving stress, in excellent accord with our thermodynamic results. In contrast to previous reports [14,15], both our longitudinal and transverse measurements were carried out on the same sample, i.e., under similar strain-transmission conditions, which is crucial for extracting the symmetry-resolved elastoresistance coefficients defined by Eqs. (1) and (2). As shown in Fig. 2(b), the enhanced elastoresistance response within the CDW phase is dominated by the symmetry-preserving A_{1g} channel. The E_{2g} response, in contrast, remains weak over the entire temperature range studied, in agreement with both the absence of in-plane C_6-symmetry breaking and the direct uniaxial-strain measurements of Qian *et al.* [29]. In light of our thermodynamic results, the large $m_{A_{1g}}$ likely originates from a dominant c-axis contribution.

Strikingly, the A_{1g}-symmetric elastoresistance increases further in the CDW phase and reaches extremely high values at low temperature, with $m_{A_{1g}}(20\ \mathrm{K}) \approx 120$, which we attribute to the strain-sensitive electron-electron scattering. Indeed, from the decrease of γ with in-plane uniaxial pressure (see Table I) and by virtue of the Kadowaki-Woods relation, $A \propto \gamma^2$ (A being the coefficient of the T^2 term in a Fermi-liquid picture), one expects the electron-electron contribution to $m_{A_{1g}}$ to be positive at low temperature [48] as effectively observed. At higher temperatures, electron-phonon scattering will play an increasingly important role in the elastoresistivity, that in turns decreases (see Ref. [26]). Finally, the downturn of the elastoresistance found below $T_{nem} \approx 35$ K [14,15,49] is a direct consequence of not accounting for the residual resistivity [48] [see open symbols in Fig. 2(a) and [26]].

In conclusion, we have demonstrated that the CDW in CsV_3Sb_5 exhibits a colossal response to c-axis stress and strongly competes with SC for the same electronic states. The simultaneous enhancement of T_c and decrease of T_{CDW} under c-axis compression is in line with the strong shift of the apical Sb-derived electronic states toward the Fermi energy [43,44], highlighting the importance of Sb-derived bands in any minimal microscopic description of this system [21,42,43]. Besides CDW and SC, we find no thermodynamic evidence of additional phase transition within the CDW state. Our data reveal the absence of an orthorhombic distortion consistent with a negligibly small $m_{E_{2g}}$ response for $T < T_{CDW}$, implying that sixfold rotational symmetry is preserved within the individual V_3Sb_5 layers. Our results remain, however, consistent with x-ray diffraction [11] if the reported breaking of C_6 invariance arises from a stacking of different CDW patterns along the c axis, as suggested theoretically in Ref. [43]. Our data further show that the large elastoresistance, previously assigned to the nematic E_{2g} channel, originates largely from an enhanced A_{1g} symmetry-preserving channel, that emerges from electron-electron scattering within the CDW phase. A careful comparison of thermodynamic and spectroscopic experiments under c-axis compression is a promising way to shed light on the microscopic origin of the CDW and SC formation in AV_3Sb_5.

Note added.—After the completion of the manuscript, we became aware of the preprints of Liu *et al.* [32] and Asaba *et al.* [50]. We share the conclusions of Liu *et al.* [32] about the absence of nematicity within the CDW state of CsV_3Sb_5. However, our thermal-expansion results and the elastocaloric measurements of Liu *et al.* [32] are at odds concerning the putative crystal-symmetry breaking well above the CDW transition reported by Asaba *et al.* [50].

We acknowledge fruitful discussions with R. M. Fernandes and M. Le Tacon. Work at KIT. was partially funded by the Deutsche Forschungsgemeinschaft (DFG, German Research Foundation) TRR 288-422213477 (Projects No. A02 and No. B03) and Chinesisch-Deutsche Mobilitätsprogamm of Chinesisch-Deutsche Zentrum für Wissenschaftsförderung (Grant No. M-0496). M. F acknowledges funding by the Alexander von Humboldt Foundation and the Young Investigator preparation program of the Karlsruhe Institute of Technology. Y. G. acknowledges the support by the National Natural Science Foundation of China (Grant No. 920651). W. X. thanks the Shanghai Sailing Program for support (23YF1426900).

*mehdi.frachet@gmail.com
†christoph.meingast@kit.edu
‡frederic.hardy@kit.edu

[1] Y. Hu, X. Wu, B. R. Ortiz, S. Ju, X. Han, J. Ma, N. C. Plumb, M. Radovic, R. Thomale, S. D. Wilson, A. P. Schnyder, and M. Shi, Rich nature of van Hove singularities in kagome superconductor CsV_3Sb_5, Nat. Commun. **13**, 2220 (2022).

[2] Maximilian L. Kiesel, Christian Platt, and Ronny Thomale, Unconventional Fermi surface instabilities in the kagome Hubbard model, Phys. Rev. Lett. **110**, 126405 (2013).

[3] M. Michael Denner, Ronny Thomale, and Titus Neupert, Analysis of charge order in the kagome metal AV_3Sb_5 (A = K, Rb, Cs), Phys. Rev. Lett. **127**, 217601 (2021).

[4] Wan-Sheng Wang, Zheng-Zhao Li, Yuan-Yuan Xiang, and Qiang-Hua Wang, Competing electronic orders on kagome lattices at van Hove filling, Phys. Rev. B **87**, 115135 (2013).

[5] Brenden R. Ortiz, Lídia C. Gomes, Jennifer R. Morey, Michal Winiarski, Mitchell Bordelon, John S. Mangum, Iain W. H. Oswald, Jose A. Rodriguez-Rivera, James R. Neilson, Stephen D. Wilson, Elif Ertekin, Tyrel M. McQueen, and Eric S. Toberer, New kagome prototype materials: Discovery of KV_3Sb_5,RbV_3Sb_5, and CsV_3Sb_5, Phys. Rev. Mater. **3**, 094407 (2019).

[6] Brenden R. Ortiz, Samuel M. L. Teicher, Yong Hu, Julia L. Zuo, Paul M. Sarte, Emily C. Schueller, A. M. Milinda Abeykoon, Matthew J. Krogstad, Stephan Rosenkranz, Raymond Osborn, Ram Seshadri, Leon Balents, Junfeng He, and Stephen D. Wilson, CsV_3Sb_5: A $\mathbb{Z}_2$ topological kagome metal with a superconducting ground state, Phys. Rev. Lett. **125**, 247002 (2020).

[7] Zuowei Liang, Xingyuan Hou, Fan Zhang, Wanru Ma, Ping Wu, Zongyuan Zhang, Fanghang Yu, J.-J. Ying, Kun Jiang, Lei Shan, Zhenyu Wang, and X.-H. Chen, Three-dimensional charge density wave and surface-dependent vortex-core states in a kagome superconductor CsV_3Sb_5, Phys. Rev. X **11**, 031026 (2021).

[8] Hengxin Tan, Yizhou Liu, Ziqiang Wang, and Binghai Yan, Charge density waves and electronic properties of superconducting kagome metals, Phys. Rev. Lett. **127**, 046401 (2021).

[9] Brenden R. Ortiz, Samuel M. L. Teicher, Linus Kautzsch, Paul M. Sarte, Noah Ratcliff, John Harter, Jacob P. C. Ruff, Ram Seshadri, and Stephen D. Wilson, Fermi surface mapping and the nature of charge-density-wave order in the kagome superconductor CsV_3Sb_5, Phys. Rev. X **11**, 041030 (2021).

[10] Qian Xiao, Yihao Lin, Qizhi Li, Xiquan Zheng, Sonia Francoual, Christian Plueckthun, Wei Xia, Qingzheng Qiu, Shilong Zhang, Yanfeng Guo, Ji Feng, and Yingying Peng, Coexistence of multiple stacking charge density waves in kagome superconductor CsV_3Sb_5, Phys. Rev. Res. **5**, L012032 (2023).

[11] Q. Stahl, D. Chen, T. Ritschel, C. Shekhar, E. Sadrollahi, M. C. Rahn, O. Ivashko, M. v. Zimmermann, C. Felser, and J. Geck, Temperature-driven reorganization of electronic order in CsV_3Sb_5, Phys. Rev. B **105**, 195136 (2022).

[12] Y. Xu, Z. Ni, Y. Liu, B. R. Ortiz, Q. Deng, S. D. Wilson, B. Yan, L. Balents, and L. Wu, Three-state nematicity and magneto-optical Kerr effect in the charge density waves in kagome superconductors, Nat. Phys. **18**, 1470 (2022).

[13] Y. Xiang, Q. Li, Y. Li, W. Xie, H. Yang, Z. Wang, Y. Yao, and H.-H. Wen, Twofold symmetry of c-axis resistivity in topological kagome superconductor CsV_3Sb_5 with in-plane rotating magnetic field, Nat. Commun. **12**, 6727 (2021).

[14] L. Nie *et al.*, Charge-density-wave-driven electronic nematicity in a kagome superconductor, Nature (London) **604**, 59 (2022).

[15] Y. Sur, K. T. Kim, S. Kim, and K. H. Kim, Optimized superconductivity in the vicinity of a nematic quantum critical point in the kagome superconductor $Cs(V_{1-x}Ti_x)_3Sb_5$, Nat. Commun. **14**, 3899 (2023).

[16] Chunyu Guo, Glenn Wagner, Carsten Putzke, Dong Chen, Kaize Wang, Ling Zhang, Martin Gutierrez-Amigo, Ion Errea, Maia G. Vergniory, Claudia Felser, Mark H. Fischer, Titus Neupert, and Philip J. W. Moll, Correlated order at the tipping point in the kagome metal CsV_3Sb_5, Nat. Phys. **20**, 579 (2024).

[17] David R. Saykin, Camron Farhang, Erik D. Kountz, Dong Chen, Brenden R. Ortiz, Chandra Shekhar, Claudia Felser, Stephen D. Wilson, Ronny Thomale, Jing Xia, and Aharon Kapitulnik, High resolution polar Kerr effect studies of CsV_3Sb_5: Tests for time-reversal symmetry breaking below the charge-order transition, Phys. Rev. Lett. **131**, 016901 (2023).

[18] Yajian Hu, Soichiro Yamane, Giordano Mattoni, Kanae Yada, Keito Obata, Yongkai Li, Yugui Yao, Zhiwei Wang, Jingyuan Wang, Camron Farhang, Jing Xia, Yoshiteru Maeno, and Shingo Yonezawa, Time-reversal symmetry breaking in charge density wave of CsV_3Sb_5 detected by polar Kerr effect, arXiv:2208.08036.

[19] Y. Xu, Z. Ni, Y. Liu, B. R. Ortiz, Q. Deng, S. D. Wilson, B. Yan, L. Balents, and L. Wu, Three-state nematicity and magneto-optical Kerr effect in the charge density waves in kagome superconductors, Nature (London) **18**, 1470 (2022).

[20] C. Mielke, D. Das, J.-X. Yin, H. Liu, R. Gupta, Y.-X. Jiang, M. Medarde, X. Wu, H. C. Lei, J. Chang, Pengcheng Dai, Q. Si, H. Miao, R. Thomale, T. Neupert, Y. Shi, R. Khasanov, M. Z. Hasan, H. Luetkens, and Z. Guguchia, Time-reversal symmetry-breaking charge order in a kagome superconductor, Nature (London) **602**, 245 (2022).

[21] Morten H. Christensen, Turan Birol, Brian M. Andersen, and Rafael M. Fernandes, Loop currents in AV_3Sb_5 kagome metals: Multipolar and toroidal magnetic orders, Phys. Rev. B **106**, 144504 (2022).

[22] C. C. Zhao, L. S. Wang, W. Xia, Q. W. Yin, J. M. Ni, Y. Y. Huang, C. P. Tu, Z. C. Tao, Z. J. Tu, C. S. Gong, H. C. Lei, Y. F. Guo, X. F. Yang, and S. Y. Li, Nodal superconductivity and superconducting domes in the topological kagome metal CsV_3Sb_5, arXiv:2102.08356.

[23] Weiyin Duan, Zhiyong Nie, Shuaishuai Luo, Fanghang Yu, Brenden R. Ortiz, Lichang Yin, Hang Su, Feng Du, An Wang, Ye Chen, Xin Lu, Jianjun Ying, Stephen D. Wilson, Xianhui Chen, Yu Song, and Huiqiu Yuan, Nodeless superconductivity in the kagome metal CsV_3Sb_5, Sci. China Phys. Mech. Astron. **64**, 107462 (2021).

[24] Ritu Gupta, Debarchan Das, Charles Hillis Mielke III, Zurab Guguchia, Toni Shiroka, Christopher Baines, Marek Bartkowiak, Hubertus Luetkens, Rustem Khasanov, Qiangwei Yin, Zhijun Tu, Chunsheng Gong, and Hechang Lei, Microscopic evidence for anisotropic multigap superconductivity in the CsV_3Sb_5 kagome superconductor, npj Quantum Mater. **7**, 49 (2022).

[25] Hui Chen *et al.*, Roton pair density wave in a strong-coupling kagome superconductor, Nature (London) **599**, 222 (2021).

[26] See Supplemental Material at http://link.aps.org/supplemental/10.1103/PhysRevLett.132.186001 and additional discussion on the elastoresistance, which includes Refs. [27]; the correspondence between single piezoelectric and uniaxial stress cell experiments, which includes Refs. [28–31]; the low temperature elastoresistance, which includes Refs. [29,32], and Refs [33–39] for the calculations of the elastic constants.

[27] M. Frachet, P. Wiecki, T. Lacmann, S. M. Souliou, K. Willa, C. Meingast, M. Merz, A.-A. Haghighirad, M. Le Tacon, and A. E. Böhmer, Elastoresistivity in the incommensurate charge density wave phase of $BaNi_2(As_{1-x}P_x)_2$, npj Quantum Mater. **7**, 115 (2022).

[28] Hsueh-Hui Kuo, Maxwell C. Shapiro, Scott C. Riggs, and Ian R. Fisher, Measurement of the elastoresistivity coefficients of the underdoped iron arsenide $Ba(Fe_{0.975}Co_{0.025})_2As_2$, Phys. Rev. B **88**, 085113 (2013).

[29] Tiema Qian, Morten H. Christensen, Chaowei Hu, Amartyajyoti Saha, Brian M. Andersen, Rafael M. Fernandes, Turan Birol, and Ni Ni, Revealing the competition between charge density wave and superconductivity in CsV_3Sb_5 through uniaxial strain, Phys. Rev. B **104**, 144506 (2021).

[30] Bruno Lüthi, *Physical Acoustics in the Solid State* (Springer, Berlin, Heidelberg, 2006).

[31] Arthur Ballato, Poisson's ratio for hexagonal crystals, Technical Report of the Army Research Laboratory, 1995, https://apps.dtic.mil/sti/pdfs/ADA293556.pdf.

[32] Zhaoyu Liu, Yue Shi, Qianni Jiang, Elliott W. Rosenberg, Jonathan M. DeStefano, Jinjin Liu, Chaowei Hu, Yuzhou Zhao, Zhiwei Wang, Yugui Yao, David Graf, Pengcheng Dai, Jihui Yang, Xiaodong Xu, and Jiun-Haw Chu, Absence of nematic instability in the kagome metal CsV_3Sb_5, arXiv:2309.14574.

[33] R. Heid and K.-P. Bohnen, Linear response in a density-functional mixed basis approach, Phys. Rev. B **60**, R3709 (1999).

[34] D. Vanderbilt, Optimally smooth norm-conserving pseudopotentials, Phys. Rev. B **32**, 8412 (1985).

[35] M. Born and K. Huang, *Dynamical Theory of Crystal Lattices* (Clarendon Press, Oxford, 1954).

[36] B. Meyer, C. Elsässer, and M. Fähnle, Fortran90 program for mixed-basis pseudopotential calculations for crystals, Max-Planck-Institut für Metallforschung, Stuttgart, 1997 (unpublished).

[37] J. P. Perdew, K. Burke, and M. Ernzerhof, Generalized gradient approximation made simple, Phys. Rev. Lett. **77**, 3865 (1996).

[38] Václav Petříček, Michal Dušek, and Lukáš Palatinus, Crystallographic computing system JANA2006: General features, Z. Kristallogr. **229**, 345 (2014).

[39] George M. Sheldrick, Crystal structure refinement with SHELXL, Acta Crystallogr. Sect. C **71**, 3 (2015).

[40] L. Zheng, Y. Wu. Zhimian, Yang, L. Nie, M. Shan, K. Sun, D. Song, F. Yu, J. Li, D. Zhao, S. Li, B. Kang, Y. Zhou, K. Liu, Z. Xiang, J. Ying, Z. Wang, T. Wu, and X. Chen, Emergent charge order in pressurized kagome superconductor CsV_3Sb_5, Nature (London) **611**, 682 (2022).

[41] K. Y. Chen, N. N. Wang, Q. W. Yin, Y. H. Gu, K. Jiang, Z. J. Tu, C. S. Gong, Y. Uwatoko, J. P. Sun, H. C. Lei, J. P. Hu, and J.-G. Cheng, Double superconducting dome and triple enhancement of T_c in the kagome superconductor CsV_3Sb_5 under high pressure, Phys. Rev. Lett. **126**, 247001 (2021).

[42] Ethan T. Ritz, Rafael M. Fernandes, and Turan Birol, Impact of Sb degrees of freedom on the charge density wave phase diagram of the kagome metal CsV_3Sb_5, Phys. Rev. B **107**, 205131 (2023).

[43] Ethan Ritz, Henrik S. Røising, Morten H. Christensen, Turan Birol, Brian M. Andersen, and Rafael M. Fernandes, Superconductivity from orbital-selective electron-phonon coupling in AV_3Sb_5, Phys. Rev. B **108**, L100510 (2023).

[44] Armando Consiglio, Tilman Schwemmer, Xianxin Wu, Werner Hanke, Titus Neupert, Ronny Thomale, Giorgio Sangiovanni, and Domenico Di Sante, Van Hove tuning of AAV_3Sb_5 kagome metals under pressure and strain, Phys. Rev. B **105**, 165146 (2022).

[45] A. E. Böhmer, F. Hardy, L. Wang, T. Wolf, P. Schweiss, and C. Meingast, Superconductivity-induced re-entrance of the orthorhombic distortion in $Ba_{1-x}K_xFe_2As_2$, Nat. Commun. **6**, 7911 (2015).

[46] L. Wang, F. Hardy, A. E. Böhmer, T. Wolf, P. Schweiss, and C. Meingast, Complex phase diagram of $Ba_{1-x}Na_xFe_2As_2$: A multitude of phases striving for the electronic entropy, Phys. Rev. B **93**, 014514 (2016).

[47] Jiun-Haw Chu, Hsueh-Hui Kuo, James G. Analytis, and Ian R. Fisher, Divergent nematic susceptibility in an iron arsenide superconductor, Science **337**, 710 (2012).

[48] P. Wiecki, M. Frachet, A.-A. Haghighirad, T. Wolf, C. Meingast, R. Heid, and A. E. Böhmer, Emerging symmetric strain response and weakening nematic fluctuations in strongly hole-doped iron-based superconductors, Nat. Commun. **12**, 4824 (2021).

[49] Note that our own measurements do also show a downturn below ≈35 K when uncorrected for the residual resistivity. See empty symbols in Fig. 2(a) and [26].
[50] T. Asaba, A. Onishi, Y. Kageyama, T. Kiyosue, K. Ohtsuka, S. Suetsugu, Y. Kohsaka, T. Gaggl, Y. Kasahara, H. Murayama, K. Hashimoto, R. Tazai, H. Kontani, B. R. Ortiz, S. D. Wilson, Q. Li, H. H. Wen, T. Shibauchi, and Y. Matsuda, Evidence for an odd-parity nematic phase above the charge density wave transition in kagome metal CsV_3Sb_5, Nat. Phys. **20**, 40 (2024).